

# Thermal Distribution based Investigations on Electromagnetic Interactions with the Human Body for Wearable Wireless Devices

Varshini Karthik<sup>1</sup> and T. R. Rao<sup>2, \*</sup>

**Abstract**—With increasing interest in the usage of wearable wireless communication technologies at 1.8 & 2.4 GHz and 5 & 8.9 GHz band of frequencies, investigations on the human body interaction with these devices are becoming important. This paper provides a microstrip-based multi-band monopole antenna for body Wearable Wireless Devices (WWD), covering licensed and license-free wireless technologies at UHF/UWB when placed on human body. Five parts of the body were considered to evaluate the electromagnetic (EM) effects on the body. Specific Absorption Rate (SAR) values were found to range from 0.09–0.25 W/kg by using numerical modeling. The thermal effects were investigated experimentally using infrared thermography, and temperature changes not exceeding 1°C were noticed. Analyses of numerical, simulated and experimental results show that infrared thermography, a temperature-based technique, can be used to evaluate the compliance of WWDs with safety exposure limits for various wireless applications.

## 1. INTRODUCTION

With exploding market for Wearable Wireless Devices (WWD), Body-Centric Wireless Communications (BCWC) show great promise for monitoring, communication in diverse application areas such as healthcare, public safety, enterprise and defence purposes via Wireless Body Area Networks (WBAN). The antenna is the crucial enabling component which allows communication between sensors and other off-body systems (e.g., GPS, GSM, 3G & 4G etc.). But the antennas that are the main source of electromagnetic (EM) radiations operate in particularly challenging environments and in close proximity to the human body. As the antenna is operated in close proximity to the body, the bio-electromagnetic effects due to the interaction of radio frequency (RF) waves with human tissues must be evaluated utilizing Specific Absorption Rate (SAR) and associated thermal effects.

In the last decade, active research has been carried out in this area. In [1] it has been established that biological effects might result from bulk temperature increase or from the rate of temperature increase. It was observed that at 3 kHz–300 GHz, biological hazards largely demonstrated were thermal in nature using experimental and theoretical dosimetry concepts of SAR [2]. Similarly in a review paper [3], it has been discussed that thermal effect is the only adverse effect of RF fields on aspects of human health. Authors in [4] after their study using simulations concluded that exposure time and environmental temperature must be one of the characteristic quantities in safety standards. Work on the SAR effects of cellular phones at 900 MHz using numerical modeling was done by [5]. In the past 5 years, immense work at various frequencies has been carried out. In 2012, study on SAR effects on human body for implanted biosensors was carried out by [6]. Numerical and experimental investigations on SAR and power density (PD) from heating dynamics on an experimental phantom at 60 GHz were done by [7]. While authors in [8] worked on bio-thermal simulations to understand SAR and thermal

---

*Received 17 July 2016, Accepted 14 September 2016, Scheduled 29 September 2016*

\* Corresponding author: Thippiraju Rama Rao (ramaraotr@gmail.com).

<sup>1</sup> Department of Biomedical Engineering, SRM University, Chennai 603203, India. <sup>2</sup> RAMS Lab, Department of Telecommunication Engineering, SRM University, India.

distributions of UWB antennas on human body, a similar work for implanted UWB antenna was carried out in [9]. Numerical estimates of SAR and thermal distribution in models for UWB frequencies at different body positions were given by [10]. The transient temperature analysis for wearable antennas at MHz frequencies was done by [11]. The most recent work in 2015 by [12] has concluded that PD is not suitable to detect exposure compliance with mm wave devices when used close to the human body. Temperature-based technique using MRI for evaluation of safety compliance has been proposed by them. However, investigations on the EM exposure compliance through use of infrared thermography, as an equivalent technique to SAR and PD measurements, covering a wide range of present and future wireless technology bands does not exist.

The present research study is designed to offer a solution for investigating the biological effects of modern day's wearable antennas from a thermal perspective. It is proposed that thermal distribution measurement using IRT (Infrared Thermography) is a simple and efficient technique that can be paralleled to SAR or PD measurements to ensure suitability and biocompatibility of wearable devices for various wireless applications. In this work, numerical modeling, using Ansys's HFSS is used to analyse the dosimetric effect of SAR. Analytical methods and experimental techniques using IR thermal camera have been adopted to evaluate the thermal effects which are direct manifestation of the EM waves.

## 2. EFFECT OF EM WAVES AND MODELING OF HUMAN TISSUES

### 2.1. Interaction of Electromagnetic Field with Human Tissues

A human body consists of different types of materials, each differing in the way that it interacts with the EM fields. The geometry of the human body and its various parts are very complex [13]. The electrical properties of the biological tissues are the result of the EM radiations interacting with constituents of the body at the cellular and molecular level [14]. Understanding the interaction and electrical properties of body tissues is the primary need for the design work of body wearable devices. For wearable devices, it is important to reduce power absorption and SAR in the design of an antenna [15]. The biological effects at UHF and UWB frequencies are proportional to the rate of energy absorption given in terms of SAR and the ability to heat human tissues. Both these effects can be hazardous if exposure is sufficiently intense or prolonged. Since the magnetic permeability of body tissues is the same as that of free space, electrical permittivity and conductivity are the important properties that determine the electric field distribution inside the body and the power dissipated in it [16]. These properties change with frequency. Tissues having the highest water content have the highest relative permittivity (e.g., skin and muscle), decreasing with increasing frequency. The tissue's water content results in specific permittivity value, which affects the wavelength inside tissues [17].

### 2.2. Layered Phantom Model of Human Tissue

For the case of wearable devices, the influences of the peripheral body tissues must be considered. There are different simplified tissue models such as homogeneous models and three-layered body models with flat, rectangular and elliptical cross sections that are available in the literature. 3D-based complex voxel body models that use lot of computational resource and time are also available. In this work, a three-layered rectangular biological tissue model made up of skin, subcutaneous adipose tissue (SAT) and muscle is chosen for computational simplicity and considerable accuracy, as it represents most of



**Figure 1.** Layered model of human tissue with antenna.

the body regions [18]. The electrical properties of the tissues at the various resonating frequencies of the designed antenna are based on the works of Italian National Research Council, which is available online [19]. Skin, due to its inhomogeneous structure, has inhomogeneous dielectric properties. Muscles and bones have intermediate dielectric properties compared to SAT which has poor dielectric properties. The designed antenna is proposed to be placed over the stacked tissues with an average thickness of 2 mm, 3.5 mm and 10 mm for skin, SAT and muscle layer respectively as shown in Fig. 1.

### 3. ANTENNA FOR WEARABLE DEVICES

#### 3.1. Antenna Requirements for Body-Centric Wireless Communications

At UHF and UWB frequencies, antennas experience resonance frequency shifts due to their proximity to the body, changes in input impedance, distortion of radiation patterns and power absorption. A proper design of wearable antennas will ensure minimum influence of the body on the performance of the antenna. The required characteristics of an antenna for on/off body communications are simplicity, low cost and small size enabling integration with a transceiver.

#### 3.2. Staircase Microstrip Patch Antenna

The antenna design requirements differ from that of a conventional antenna designed for free space because of the tissue environment. Fig. 2 shows a photograph of the prototype of a staircase microstrip antenna. Microstrip model design equation [20] was used to design the antenna. The antenna has a dimension of  $35 \times 32 \times 1.57 \text{ mm}^3$  and is made of a Rogers RT/Duroid 5880 substrate with relative permittivity of 2.2 and loss tangent of  $9 \times 10^{-3}$ . The antenna with a partial ground plane and rectangular staircase patch is used for an optimized design. The step size of 1 mm followed by 1.5 mm from both the top and bottom edges is used for the staircase pattern, and a  $50 \Omega$  microstrip line feeds the radiating patch with 1.0 mW as input power. A microstrip tapered line is used for proper impedance matching and conducting material at the bottom of the substrate provides a defected ground plane.

The design is optimized to make the antenna work at two UHF and UWB frequencies with return loss less than  $-10 \text{ dB}$ . A defected ground plane helps to achieve the multiband operation of the antenna. The slots on the patch align the shifted bands to the required resonant frequencies, and the steps offer a greater value of return loss at all the frequencies. A multi-band operation is chosen to provide better EM compatibility with existing wireless communication technologies and unlicensed UWB band so that it can be used for both low and high data rate wireless applications.

## 4. SIMULATION AND EXPERIMENTAL RESULTS

#### 4.1. Simulation and Measurement Results for Antenna Placed on Body

The antenna is simulated as well as measured for its performance on-body. Measurements of return loss were made for the prototype antenna using Keysight's RS-ZVL Vector Network Analyzer of frequency range 9 kHz–13.6 GHz. Placement of the antenna in direct contact with the body decreases the gain and radiation efficiency with due effects on the impedance matching due to the dielectric loading provided by the lossy human tissues. The designed antenna is kept on the human body with cotton padding of 5 mm between them. The performance of the antenna on the body is enhanced due to the bio and electromagnetic compatibility nature of the chosen fabric which makes it realizable for real-time use compared to the few mm of air gap used in previous designs. It is observed that there is good agreement between the simulated and measured results, and they are plotted in Fig. 3.

The radiation patterns of the antenna in free space, considering the thickness of the layers of skin, SAT and muscle as 2, 3.5, 10 mm respectively at the four frequencies, are shown in Fig. 4. The back radiation into the body is reduced in the  $H$  plane. The performance of the multi-bands is studied and tabulated in Table 1. It is seen from the table that the upper frequencies perform well compared to the lower frequencies which is important while considering the EM waves (thus antennas as well) interaction with the body [10]. Primary reflections occur due to the wave impedance mismatch between low (fat) and high water content (skin, muscle) tissues. For higher GHz frequencies, the radiations are absorbed

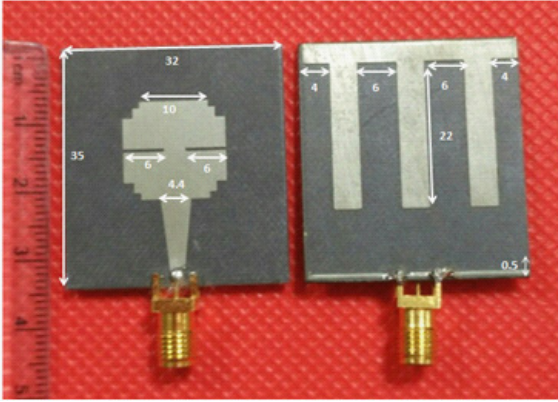


**Figure 2.** Photograph of the prototype of staircase microstrip antenna with the dimensions in mm for radiating patch and ground plane respectively.

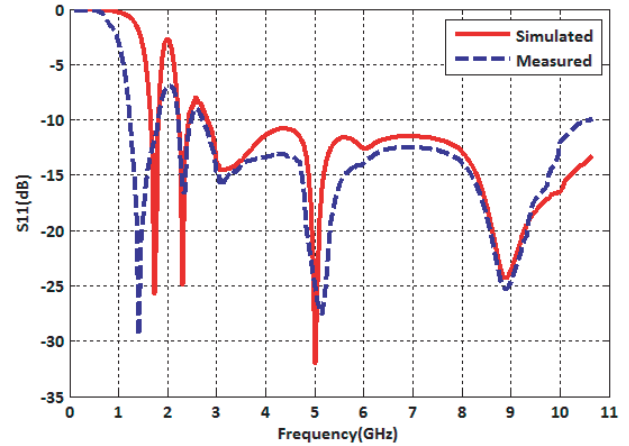


**Figure 3.** Simulated and measured return loss plot for on body placement of the antenna.

less by the body, hence reflections are making the antenna radiate more efficiently. This leads to a decrease in SAR as frequency increases [18]. The general trend of radio waves permittivity into body tissues is that as frequency increases, permittivity decreases. This leads to better reflections away from the body and hence increase in radiation efficiency. But at GHz in UWB range, along with the trend stated above there is an additional effect of directivity. In the UWB frequency ranges, as frequency increases, the directivity increases due to reflection of propagation waves from the body. With not much difference in gain values, the increase in directivity decreases the radiation efficiency at higher UWB frequencies [21].

#### 4.2. SAR and Thermal Effects at Five Body Sites

SAR is a good dosimetric quantity that measures the rate of energy absorption by human body tissues when exposed to radio frequency EM field. SAR is calculated as:

$$\text{SAR} = \frac{\sigma \cdot |E|^2}{\rho_m} \quad (1)$$

Here,  $E$  is the RMS value of induced field in (V/m),  $\sigma$  the conductivity of tissue in (S/m), and  $\rho_m$  the mass density of tissue in  $\text{kg/m}^3$ . The antenna is analysed for its SAR in the body through simulations for the four bands at various tissues at five different anatomical sites on the body, shown in Fig. 5. The tissue layer thickness is tabulated in Table 2 keeping muscle thickness at 10 mm. The various body parameters considered for SAR and temperature calculations are listed in Table 3. The SAR values were found to be far less than the maximum allowable limit of 2 W/kg averaged over 10 g of tissue exposed to EM radiations given by International Council on Non-Ionizing radiation protection [22] and 1 g averaged SAR value of 1.6 W/Kg given by IEEE/ICES C95.1-2005 [23].

**Table 1.** Performance of multi-frequencies in free space and on body.

Performance Metrics/Quad Band	Total Gain (dB)		Radiation efficiency (%)		Total efficiency (%)	
	Free Space	On Body	Free Space	On Body	Free Space	On Body
1.8 GHz	2.7	-6.7	98	8.30	97.5	8.02
2.4 GHz	3.2	-1.3	98	16.3	97.9	16.1
5.0 GHz	7.0	5.1	99	57.4	98.8	57.3
8.9 GHz	6.8	5.0	99	49.2	98.8	48.9

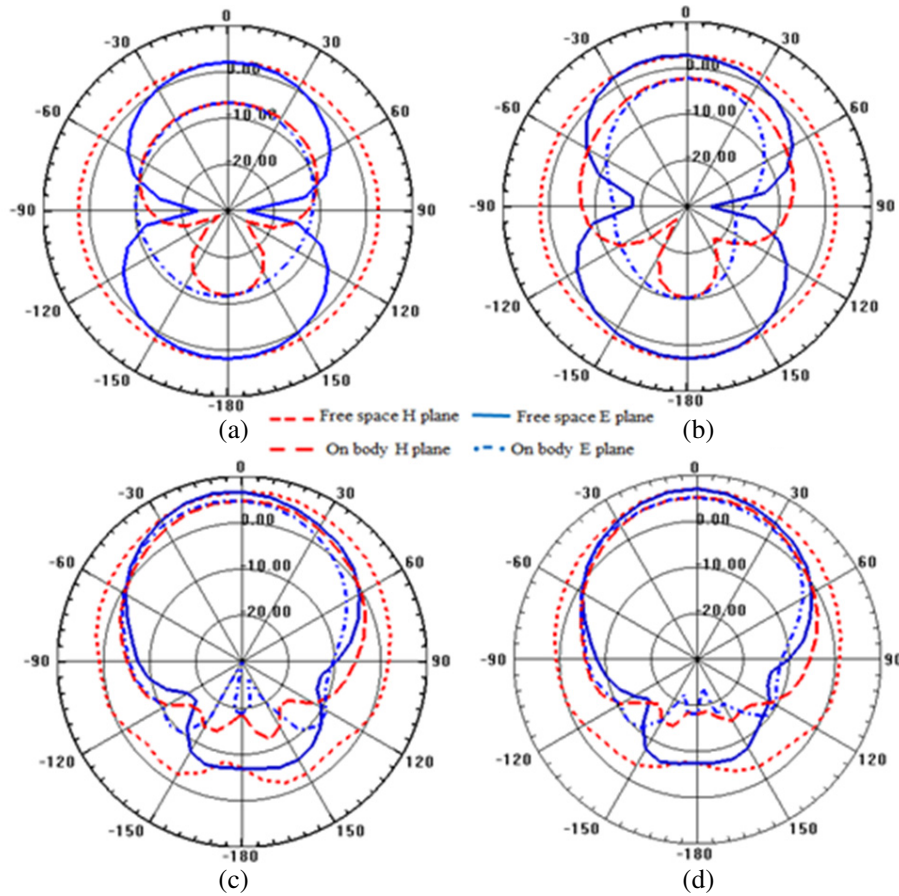
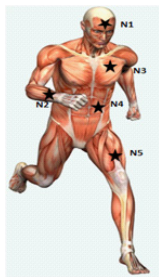


**Figure 4.** Simulated radiation pattern of the antenna showing gain (dB) for the quad bands, (a) 1.8 GHz, (b) 2.4 GHz, (c) 5 GHz, (d) 8.9 GHz, when the proposed antenna is placed in free space and on body.



Node	Anatomical Site	Skin Thickness (mm)	SAT Thickness (mm)
N1	Forehead	1.05	3.05
N2	Forehead	0.60	0.9
N3	Chest	2.00	3.1
N4	Abdomen	2.30	10
N5	Thigh	1.87	5.6

**Figure 5.** Anatomical sites of the body considered for simulations. **Table 2.** Tissue thickness at five body sites.

Adiabatic conditions are assumed for heat exchange with the environment which gives the worst case temperature increase [24] in a state where no heat is exchanged with the environment. To obtain the relation between rise in temperature and time, in the case of long time exposures, the Pennes bio heat equation has been used [25]. Simplifying the bio heat differential equation yields Eq. (2) [25] that gives the maximum temperature rise over an extended period of time in the order of minutes. In the equation,  $S$  is average SAR in W/kg,  $\rho$  the mass density of tissue in kg/m<sup>3</sup>,  $K$  the thermal conductivity of the tissues in W/m/K,  $\rho_b$  the mass density of blood in kg/m<sup>3</sup>,  $c_b$  the heat capacity of blood in J/kg/K,  $c$  the heat capacity of the tissue in J/kg/K,  $w$  the blood perfusion rate in ml/g/min, and  $\lambda$  the

wavelength of the EM wave in m. Using SAR values tabulated in Table 4, the maximum temperature rise for the different tissues at all the four frequencies are tabulated using Eq. (2) in Table 5.

$$T_{max} = \frac{q}{\lambda'} \left[ 1 - \left( \sqrt{\lambda'} A + 1 \right) e^{-\sqrt{\lambda'} A} \right], \quad \text{where,} \quad q = \frac{\rho S}{K}; \quad \lambda' = \frac{w c_b}{K}; \quad A = \frac{\lambda}{4} \quad (2)$$

### 4.3. Transient Temperature Analysis for Long Term Exposure

Transient analysis of the temperature rise in the time domain is the most interesting part. There are two different approaches depending on whether the distance (radius) of the tissue at a body region is smaller or greater than the wavelength considered. When Equation (3) [25] is plotted, considering the different body tissues and various parameters in Table 3, the time evolution of the rise of temperature for long time exposure of a few minutes to hours is obtained. To investigate the long-term temperature effect of the designed antenna, the transient analysis is done for a scenario when the antenna is placed on the forearm and excited at the four frequencies with an input power of 1 mW. The rise in temperature with time is plotted using Matlab tool using Eq. (3) which is the second approach to the transient case where distance (radius  $R$  of the forearm tissue) is greater than a quarter wavelength. Time evolution of the temperature rise in different tissues at the four resonant frequencies is plotted in Fig. 6, and it is observed that the maximum temperature rise is on the skin compared to SAT or muscle. This is in a manner conforming to skin having greater temperature rise at all the five body parts as observed in Table 5. At resonating frequencies of 1.8 and 2.4 GHz, muscle tissue has greater temperature rise than fat tissue as fat is a very poor absorber of EM waves. At higher frequencies of 5 GHz and 9 GHz, depth of EM wave penetration inside the tissues becomes less. The smaller the wavelength is, the lower the penetration is. Hence, the EM waves reaching the muscle become less, and the temperature rise in the muscle tissue equals or remains less than the increase in fat tissues as seen in Fig. 6. The time evolution of temperature for the four tissues obtained shows that after an initial increase in temperature, there is saturation in the graph owing to the physiological aspects of the thermoregulation of the body primarily

**Table 3.** Parameter values of body tissues.

Tissue/Parameter	Mass density (kg/m <sup>3</sup> )	Thermal conductivity (W/m/K)	Heat capacity (J/kg/K)
Skin	1109	0.37	3391
Fat	911	0.21	2348
Muscle	1090	0.49	3421

**Table 4.** Average SAR values at four frequencies at different body sites.

Average SAR 10 <sup>-2</sup> (W/kg)												
Tissue/ Nodes	Skin				Fat				Muscle			
	1.8 GHz	2.4 GHz	5.0 GHz	8.9 GHz	1.8 GHz	2.4 GHz	5.0 GHz	8.9 GHz	1.8 GHz	2.4 GHz	5.0 GHz	8.9 GHz
N1-Forehead	22	20	17	15	2.5	2.1	1.7	1.5	5.4	3.4	1.6	0.8
N2-Forearm	25	16	15	11	1.5	1.3	1.2	1.0	4.4	3.9	1.4	0.4
N3-Chest	17	14	13	10	1.3	1.2	0.9	0.9	4.4	3.2	1.5	0.4
N4-Abdomen	22	17	16	9.0	1.1	0.9	0.9	0.6	1.2	1.2	0.3	0.1
N5-Thigh	21	17	13	10	1.1	1.1	1.0	0.8	2.8	2.6	0.8	0.3

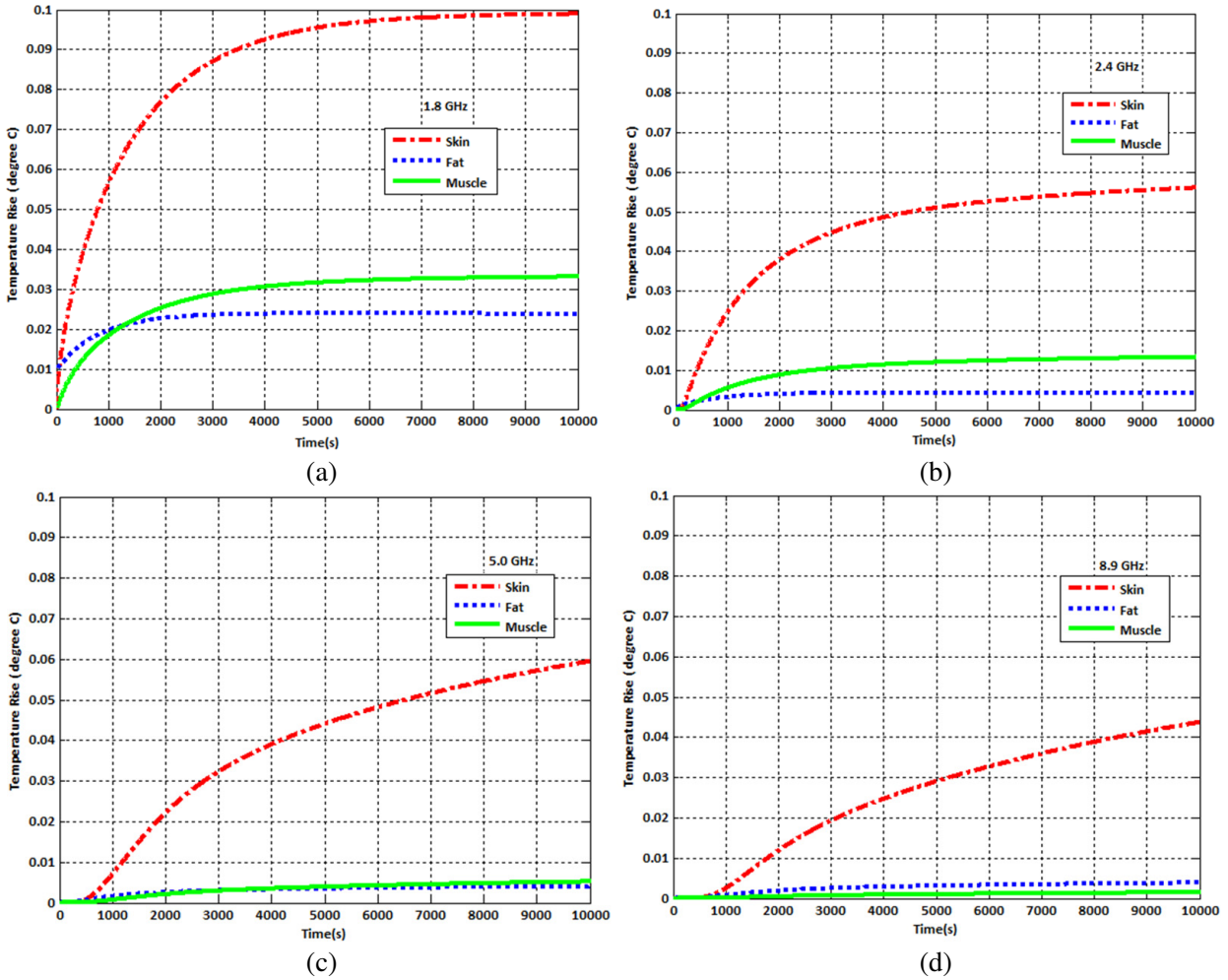


**Figure 6.** Time evolution of the temperature rise in different tissues at the four resonant frequencies.

due to blood flow.

$$\begin{aligned}
 T(t) = & \frac{q}{2\lambda'} \frac{\rho}{r} \left\{ \frac{e^{(r-\rho)}}{2} \left(1 + \frac{1}{\rho}\right) \cdot \operatorname{erfc}\left(\frac{r-\rho}{2\sqrt{\tau}}\right) + \frac{e^{-(r-\rho)}}{2} \left(1 - \frac{1}{\rho}\right) \cdot \operatorname{erfc}\left(\frac{r-\rho}{2\sqrt{\tau}} - \sqrt{\tau}\right) \right. \\
 & + \frac{e^{(r+\rho)}}{2} \left(1 - \frac{1}{\rho}\right) \cdot \operatorname{erfc}\left(\frac{r+\rho}{2\sqrt{\tau}} + \sqrt{\tau}\right) + \frac{e^{-(r+\rho)}}{2} \left(1 + \frac{1}{\rho}\right) \cdot \operatorname{erfc}\left(\frac{r+\rho}{2\sqrt{\tau}} - \sqrt{\tau}\right) \\
 & \left. + \frac{r}{\rho} e^{-\tau} \left[ \operatorname{erfc}\left(\frac{r+\rho}{2\sqrt{\tau}}\right) - \operatorname{erfc}\left(\frac{r-\rho}{2\sqrt{\tau}}\right) + \frac{2}{\rho} \sqrt{\frac{\tau}{\pi}} \left( \exp\left(-\frac{(r-\rho)^2}{4\tau}\right) - \exp\left(-\frac{(r+\rho)^2}{4\tau}\right) \right) \right] \right\} \quad (3)
 \end{aligned}$$

where,  $\rho = \sqrt{\lambda'} A$ ;  $\tau = \frac{\lambda'}{\mu} t$ ;  $r = \sqrt{\lambda'} R$ ;  $\mu = \frac{\rho C}{K}$ ;  $\operatorname{erfc}(x) = 1 - \frac{2}{\sqrt{\pi}} \int_0^x e^{-t^2} dt$ .

#### 4.4. Experimental Validation of on Body Thermal Effect of the Antenna

Infrared Thermography (IRT) is an imaging modality using which the variations in temperature in human beings can be measured. An experimental setup to validate the thermal effects of the designed antenna was made with healthy subjects with the region of interest at a distance of 1 m from the IR camera. Thermo-grams were taken against a dark non-reflecting background using FLIR A305SC series IR camera and analyzed using FLIR R&D research IR software tool. The images were captured and analyzed under normal body condition of the subject with no particular regards to hormonal, metabolic,

**Table 5.** Maximum temperature rise at four frequencies at different body sites using bio-heat equation.

Maximum temperature rise $10^{-2}$ ( $^{\circ}\text{C}$ )												
Tissue/ Nodes	Skin				Fat				Muscle			
	1.8 GHz	2.4 GHz	5.0 GHz	8.9 GHz	1.8 GHz	2.4 GHz	5.0 GHz	8.9 GHz	1.8 GHz	2.4 GHz	5.0 GHz	8.9 GHz
<b>N1-Forehead</b>	13.4	12.2	10.4	9.1	1.25	1.05	0.85	0.75	3.3	2.10	0.98	0.53
<b>N2-Forearm</b>	15.0	9.61	9.19	6.74	0.75	0.75	0.60	0.50	2.71	2.40	0.86	0.28
<b>N3-Chest</b>	10.4	8.58	7.97	6.13	0.65	0.60	0.48	0.47	2.79	1.97	0.92	0.27
<b>N4-Abdomen</b>	13.1	10.0	9.8	5.5	0.55	0.49	0.48	0.33	0.74	0.74	0.20	0.06
<b>N5-Thigh</b>	12.8	10.4	7.9	6.1	0.55	0.55	0.55	0.40	1.71	1.60	0.51	0.21

**Table 6.** Thermal effect due to on-body antenna for various durations as observed from thermograms.

Frequency (GHz)	Average temperature rise ( $^{\circ}\text{C}$ ) for 1 mW power level		
	10 minutes	20 minutes	30 minutes
<b>1.8</b>	0.2	0.6	0.6
<b>2.4</b>	0.1	0.4	0.4
<b>5.0</b>	0.1	0.3	0.3

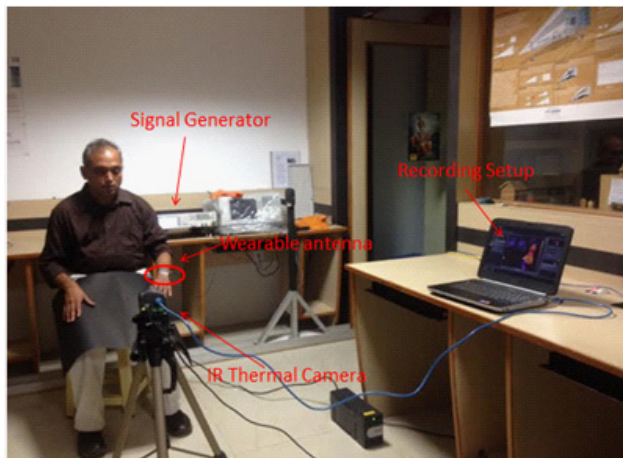


**Figure 7.** Experimental set up to study the thermal effect of the wearable antenna.

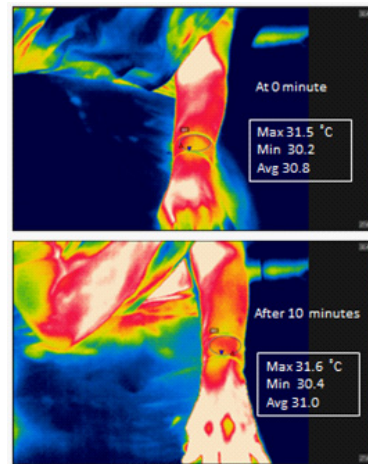


**Figure 8.** Sample thermo gram at 0 and 10 minutes of emission from the wearable antenna on the forearm at 1.8 GHz.

digestive and drug effects. For the marked area of interest, thermo-grams were taken on the forearm, revealing the skin temperature before placing the antenna and exciting it. The antenna was excited at 1.8, 2.4 and 5 GHz at 1.0 mW power level by Keysight’s N5182A MXG vector signal generator. The experimental setup to study the thermal effect of the wearable antenna is shown in Fig. 7. After duration of 10, 20, and 30 minutes emission from the antenna placed on the body, thermo-grams were obtained, a sample of which is shown in Fig. 8. The temperature rise in degree Celsius was analysed on the skin as it is the tissue that has maximum temperature rise as found from Table 5. Utilizing the thermograms, temperature rise for different durations is tabulated in Table 6. The increment in temperature observed using thermal investigations has a positive correlation with a correlation coefficient of 0.97, with those obtained through numerical analysis (Table 5) using simulated values of SAR in Table 4.

## 5. DISCUSSIONS AND CONCLUSIONS

This research work investigates the interactions and implications of the human body and wireless communication systems at 1.8 & 2.4 GHz and 5 & 8.9 GHz frequencies. The performance and body interactions of a multiband microstrip monopole antenna for WWDs are investigated when it is placed on a human body. The effect of the human body on the performing antenna is studied with regard to return loss, total gain, radiation efficiency, total efficiency and radiation pattern of the antenna. The effect of the performing antenna on the human body is studied regarding SAR and thermal effects at five different body sites of varying tissue layer thicknesses for all the multi-frequencies. The SAR value of skin which is the outermost layer was maximum ranging from 0.09–0.25 W/kg. Decreased permittivity with increase in frequency in the GHz range causes better reflections away from the body which results in less absorption by the body and hence lower SAR at higher frequencies. This in turn reduces the heating effects which are the biological manifestation of SAR. The maximum achieved temperature change is on the skin with the highest for 1.8 GHz and is of value 0.15°C, 0.1°C, 0.1°C as obtained from numerical modeling, transient analysis and experimental method using IRT respectively. Thermal values within safety exposure guidelines of 1°C make the proposed antenna compliant with international safety regulations, favoring the use of the antenna for wearable devices. It is comprehended that IRT is a simple temperature dependent technique that can be paralleled to other methods to test the EM compatibility of wearable devices.

## REFERENCES

1. Foster, K. R., "Thermal and nonthermal mechanisms of interaction of radio-frequency energy with biological systems," *IEEE Transactions on Plasma Science*, Vol. 28, No. 1, 15–23, 2000.
2. Adair, E. R. and R. C. Petersen, "Biological effects of radiofrequency/microwave radiation," *IEEE Transactions on Microwave Theory and Techniques*, Vol. 50, No. 3, 953–962, 2002.
3. Chou, C.-K. and J. A. D'Andrea, "Reviews of effects of RF fields on various aspects of human health: Introduction," *Bioelectromagnetics*, Vol. 24, No. S6, S5–S6, 2003.
4. Nikolaeva, E. Y., et al., "Analysis of thermal effects in human exposed to EM radiation (2D case)," *Proceedings of the 9th International Seminar/Workshop on IEEE Direct and Inverse Problems of Electromagnetic and Acoustic Wave Theory, DIPED 2004*.
5. Ibrahim, A., et al., "Analysis of the temperature increase linked to the power induced by RF source," *Progress In Electromagnetics Research*, Vol. 52, 23–46, 2005.
6. Soontornpipit, P., "Effects of radiation and SAR from wireless implanted medical devices on the human body," *Journal of the Medical Association of Thailand*, Vol. 95, S189–97, 2012.
7. Zhadobov, M., N. Chahat, R. Sauleau, C. Le Quement, and Y. Le Drean, "Millimeter-wave interactions with the human body: state of knowledge and recent advances," *International Journal of Microwave and Wireless Technologies*, Vol. 3, No. 2, 237–247, 2011.
8. Tuovinen, T., et al., "On the evaluation of biological effects of wearable antennas on contact with dispersive medium in terms of SAR and bio-heat by using FIT technique," *International Symposium on IEEE Medical Information and Communication Technology (ISMICT)*, 49–153, Tokyo, Mar. 6–8, 2013.
9. Thotahewa, K., J.-M. Redouté, and M. R. Yuce, "SAR, SA, and temperature variation in the human head caused by IR-UWB implants operating at 4 GHz," *IEEE Transactions on Microwave Theory and Techniques*, Vol. 61, No. 5, 2161–2169, 2013.
10. Fadhel, B. S. and M. R. Kamarudin, "EM wave effects upon the human body using UWB antennas," *Journal of Info and Electronics Engineering*, Vol. 4, No. 2, 158, 2014.
11. Francesc, S., "Radiation effects of wearable antenna in human body tissues [dissertation]," University of Colorado Springs, 2014.
12. Wu, T., T. S. Rappaport, and C. M. Collin, "Safe for generations to come: Considerations of safety for millimeter waves in wireless communications," *IEEE Microwave Magazine*, Vol. 16, No. 2, 65–84, 2015.

13. Siauve, N., R. Scorretti, N. Burais, L. Nicolas, and A. Nicolas, "Electromagnetic fields and human body: A new challenge for the electromagnetic field computation," *The International Journal for Computation and Mathematics in Electrical and Electronic Engineering*, Vol. 22, No. 3, 457–469, 2003.
14. Gabrie, C. G. and S. Corthout, "The dielectric properties of biological tissues: I. Literature Survey," *Phys. Med. Biol.*, Vol. 41, 2231–2249, 1996.
15. Anguera, J., A. Andújar, C. Picher, L. González, C. Puente, and S. Kahng, "Behavior of several antenna topologies near the human head at the 2.4–2.5 GHz band," *Microwave and Optical Technology Letters*, Vol. 54, No. 8, 1911–1916, Aug. 2012.
16. Hernandez, S. and A. David, *High Frequency Electromagnetic Dosimetry*, Artech House Inc., 2009.
17. Tuovinen, T., M. Berg, K. Y. Yazdandoost, and J. Iinatti, "Ultra wideband loop antenna on contact with human body tissues," *IET Microwave and Antennas Propagation*, Vol. 7, No. 7, 588–596, 2013.
18. Klemm, M. and G. Troester, "EM energy absorption in the human body tissues due to UWB antennas," *Progress In Electromagnetics Research*, Vol. 62, 261–280, 2006.
19. Italian National Research Council, Institute for Applied Physics, homepage on Dielectric properties of body tissues, [Online], Available: <http://niremf.ifac.cnr.it>.
20. Ramesh, G., P. Bhartia, I. Bahl, and A. Ittipiboon, *Microstrip Antenna Design Handbook*, Artech House, 2001.
21. Hall, P. S. and Y. Hao, *Antennas and Propagation for Body-centric Wireless Communications*, 2nd Edition, Artech House, 2012.
22. ICNIRP Guidelines for limiting to time varying electric, magnetic, and electromagnetic fields (upto 300 GHz), *Health Physics*, Vol. 74, No. 4, 494–522, 1998.
23. IEEE Standard for Safety Levels with Respect to Human Exposure to the Radio Frequency Electromagnetic Fields, 3 kHz to 300 GHz. IEEE Std. C95.1. 2005.
24. Samaras, T., A. Christ, A. Klingeböck, and N. Kuster, "Worst case temperature rise in a one-dimensional tissue model exposed to radiofrequency radiation," *IEEE Trans. on Biomedical Engineering*, Vol. 54, No. 3, 492–496, 2007.
25. Kritikos, H. N. and H. P. Schwan, "Potential temperature rise induced by electromagnetic field in brain tissues," *IEEE Trans. on Biomedical Engineering*, Vol. 26, No. 1, 29–34, 1979.